

## Article

# Contribution of Spring Snowmelt Water to Soil Water in Northeast China and Its Dynamic Changes

Wenshuai Zhang <sup>1</sup>, Chen Du <sup>1</sup>, Lijuan Zhang <sup>1,\*</sup>, Yulong Tan <sup>2</sup>, Yutao Huang <sup>1</sup> and Meiyi Jiang <sup>1</sup>

<sup>1</sup> Heilongjiang Province Key Laboratory of Geographical Environment Monitoring and Spatial Information Service in Cold Regions, Harbin Normal University, Harbin 150025, China; vincentzhang1993@gmail.com (W.Z.); dorisdu0911@163.com (C.D.); huangyutao0128@163.com (Y.H.); jiangmi199608@163.com (M.J.)

<sup>2</sup> Heilongjiang Province Hulin Meteorological Bureau, Hulin 154300, China; hlqxytl@163.com

\* Correspondence: zhlij@hrbnu.edu.cn

**Abstract:** Snowmelt water in spring is an important source of soil water, which is critical to supporting crop growth. Quantifying the contribution of snowmelt water to soil water and its dynamic changes is essential for evaluating soil moisture and allocating agricultural water resources. In this paper, through controlled outdoor experiments, different snow depths and soil depth gradients were set; and snow, precipitation, and soil samples were collected regularly. To analyze the contribution of snowmelt water to soil water and its dynamic changes, the MAT-253 stable isotope ratio mass spectrometer was adopted for hydrogen and oxygen isotope analyses. The results showed that the snowmelt water for snow depths of 10 cm, 30 cm, and 50 cm all contributed to the 0–30 cm soil layer. The contribution increased with soil depth, contributing 8.13%, 8.55%, and 11.24%, respectively. The contribution of the snow cover at the same depth to the soil moisture at different depths also varied, i.e., the contribution increased with increasing soil depth. The snowmelt water retention time at depths of 10 cm, 30 cm, and 50 cm was inconsistent, i.e., it was the longest at 0–10 cm (average of 69 days), followed by 20–30 cm (average of 59 days), and the shortest at 10–20 cm (average of 54 days). The greater the snow depth, the shorter the retention time of the snowmelt water in the different soil layers. For surface soil, the contribution of the snowmelt water at greater depths was significantly different; while for deep soil, the contribution was more sensitive to the snow depth. Regardless of snow depth, soil contributions at different depths were significantly different. Precipitation also affected the contribution of the snowmelt water to the soil water, exhibiting different effects at different depths.

**Keywords:** hydrogen and oxygen isotopes; snowmelt water; soil water; contribution



**Citation:** Zhang, W.; Du, C.; Zhang, L.; Tan, Y.; Huang, Y.; Jiang, M. Contribution of Spring Snowmelt Water to Soil Water in Northeast China and Its Dynamic Changes. *Water* **2022**, *14*, 1368. <https://doi.org/10.3390/w14091368>

Academic Editor: Hongyi Li

Received: 8 March 2022

Accepted: 15 April 2022

Published: 22 April 2022

**Publisher's Note:** MDPI stays neutral with regard to jurisdictional claims in published maps and institutional affiliations.



**Copyright:** © 2022 by the authors. Licensee MDPI, Basel, Switzerland. This article is an open access article distributed under the terms and conditions of the Creative Commons Attribution (CC BY) license (<https://creativecommons.org/licenses/by/4.0/>).

## 1. Introduction

The issue of water resources has been a major topic in China and globally [1]. As a special source of water resources, snowmelt water plays an increasingly important role [2]. Northeastern China, the region with the largest snow accumulation among the three major snow regions in China, generates a huge amount of snowmelt water in spring [3]. Northeastern China is an important grain production area, and its food security remains a concern [4]. The soil moisture during spring sowing affects the development of the seedlings and grain yield [5]. In recent years, frequent spring droughts have reduced grain production in this region [6,7]. Since snowmelt water is the main source of spring soil water in northeastern China, exploring its contribution to soil water and its dynamic changes regarding soil water provides important guidance for soil moisture assessment and agricultural water resource allocation [8,9]. However, few related studies have been conducted on these topics.

Hydrogen and oxygen stable isotopes of water are natural trackers, which are widely used in hydrological tracking. Due to the stability of chemical properties and their con-

sistent behavior with water migration, the stable isotopes of D and  $^{18}\text{O}$  have become important indicators that can represent the information of hydrological processes. They are used to quantitatively evaluate water evaporation and connectivity and conversion rates between different water bodies in a watershed [10,11] and to determine the contribution of different recharge sources in mixed water bodies [12–18]. Isotopic tracers can also help assess runoff sources on annual and seasonal time scales [19–21], estimate the contribution of glacial snowmelt water and frozen soil water to runoff [22], determine the importance of snowmelt to groundwater recharge [23], and evaluate the hydrological processes controlling lake water balance [24]. In addition, isotope tracers have also been applied in qualitative and quantitative identification and source diagnosis of water salinization, showing good application value [25–27]. In terms of using an isotope tracer to study the interaction between groundwater and surface water, Dincer et al. used environmental isotope technology to conduct tracer experiments in small mountainous basins in northern Czechoslovakia [28]. They showed that groundwater often affects snowmelt runoff in humid to sub humid areas. Fritz et al. and Sklash studied the environmental isotopes of eight watersheds with different hydrogeology in Canada and found that there were a large number of groundwater components in rainstorm and snowmelt runoff [29,30]. Gui et al. conducted stable isotope tracing on 202 samples of precipitation, permafrost water, river water, groundwater and soil water in the Qinghai Tibet Plateau from 2013 to 2014 [31]. It was found that the river water in the Anyuan River Basin in the northeast of the Qinghai Tibet Plateau mainly comes from precipitation and permafrost water, of which the average contribution rates of permafrost water and precipitation to the river water in the basin are 24% and 76%, respectively. Based on the study of stable isotopes, the changes of stable isotopes in different water areas during the year show that the transformation modes of surface water and groundwater are different [32].

The quantitative analysis of the contribution of different water sources to mixed water is often carried out by EMMA (End member mixing analysis model). Based on the tracer test data and the law of mass conservation, Sklash et al. proposed a method to determine the source proportion of mixed water, which is called EMMA [33]. Hooper et al. and Hooper introduced the EMMA based on chemical isotopes to analyze the composition of water [34,35]. Since then, EMMA has been widely used. Different scholars often use two-dimensional EMMA and three-component EMMA to analyze the effect of potential water sources on water flow, quantify the contribution of potential sources and the interaction between different water bodies. For example, stable isotopes are used to determine the water source of precipitation [36–38], river water [39], glacier melt water [40], lake water [41], groundwater [42,43], and explore the impact of surface water or other water sources on groundwater. Chen et al. and Li et al. further proposed that hydrogen and oxygen stable isotopes are the most commonly used two-component hydrographic separation tracers [44,45]. Therefore, using stable isotopes of hydrogen and oxygen from different sources and using EMMA, the in situ and contribution rate of mixed water can be calculated.

Soil water can be easily changed by various factors, such as precipitation, evaporation, topography, surface temperature, wind speed, biological absorption, and utilization [46], making it difficult to grasp the changes in the amount of soil water and the spatial distribution with time at different scales [47]. Several existing studies have investigated the quantity and physicochemical properties of soil water [48]. For example, Zhang et al. [49] analyzed the stable hydrogen and oxygen isotopes of soil water in the water source area of the Yuanyang terraces and reported that the isotope values had large fluctuation ranges in the surface soil profile and the fluctuation range of  $\delta^{18}\text{O}$  decreased with increasing soil depth (without quantitative analysis). Wu et al. used stable hydrogen and oxygen isotope analyses to measure the isotopic distribution characteristics of soil water and condensate water under the membrane [50]. Results showed that  $^{18}\text{O}$  was enriched in condensation water and its enrichment was much larger than that in surface soil which resulted from evaporation. In the Zhongliang Mountain in the Beibei District of Chongqing City, Wu et al.

used stable isotope analysis to study temporal and spatial variation characteristics of the hydrogen and oxygen isotopes of soil water in the 0–15 cm and 15–45 cm soil profiles under different land use patterns [51]. The results indicated that precipitation is the main source of the soil water supply in this area. The seasonal variations of  $\delta D$  and  $\delta^{18}O$  of the soil water are significant in different months of the rainy season, but there is no significant difference in the soil water  $\delta D$  and  $\delta^{18}O$  under different land use patterns. By studying the seasonal variations in the oxygen isotopes of the soil water at two locations in Washington state, Robertson et al. showed that from summer to winter, the isotopic values of the shallow soil water were higher than those of the deep soil water; while the isotopic values of the shallow and deep soil water were similar during the snow melting period in spring [52].

At present, few quantitative studies have been conducted on the contribution of snowmelt water to soil water in China and abroad. Most previous studies focused on qualitative description and analysis. For this type of research, the existing method is mainly to determine the amount of soil water and its energy state through experiments, such as monitoring the soil water content in the field and calculating the soil water flux. For example, based on snow cover test, Fu et al. suggested that during the snow melting period, the infiltration of snowmelt water inhibited a steady increase in soil temperature, and the water content increased suddenly [53]. The soil water content gradually increased with increasing snow depth [54]. By analyzing the relationship between the snow cover and soil moisture in northern China, Lu et al. proposed that snow cover caused the uniform fluctuations in the soil water content of each layer over time, which signified the time-lagged effect of soil water infiltration. They reported that snow cover was conducive to maintaining the stability of the soil water content and to increasing soil water content [55]. Liang concluded that winter snow cover on farmland is significantly correlated with soil water content in spring [56]. Možný reported that the duration and thickness of the snow cover significantly affected the soil water content in the late growth stage [57]. The limitations of the above studies were that they only measured the macroscopic changes in the soil moisture, but failed to reveal the contribution of the snow cover to the soil water content. As a result, they did not determine its specific source and destination [58]. In 1953, Dansgaard studied the  $^{18}O$  characteristics of atmospheric precipitation [59]. After this, the geochemical method based on stable hydrogen and oxygen isotopes gradually became standard in related water research, which opened up new opportunities for gaining an in-depth understanding of soil water migration and transformation mechanisms [60]. Briefly, the geochemical method utilizes the indicative function of the stable hydrogen and oxygen isotopes of water molecules [60,61] to investigate the migration of the soil water by tracking the migration of stable isotopes; ultimately, the pattern of the soil water migration can be studied at different spatial scales [62]. Gazis et al. used the changes in the isotopic values in different soil layers to obtain information about the water migration in the soil and analyzed the properties, sources, and consumption and migration patterns of soil water at the microscopic level [63].

Previous studies on the isotopes of soil water mostly concentrated on the qualitative description and the distribution characteristics, which can be affected by the extraction technique. The research on isotopes in soil water mostly focuses on qualitative description and distribution characteristics, and due to the influence of extraction technology, the overall research progress is still relatively slow. Studies on the quantitative analysis of soil water quantities are still very rare. Therefore, based on controlled outdoor experiments, in this study, the quantitative relationship between the contribution of the snowmelt water to the soil water in spring was explored. The results of this study will provide a quantitative basis for a scientific understanding of the impact of snow melt water on soil moisture, and provide a scientific basis for studying the effects of snow cover changes.

## 2. Materials and Methods

### 2.1. Experimental Site

The experimental site was located in Yichun City, Heilongjiang Province, China. Heilongjiang Province is in the highest latitude region in China. It has cold temperate and temperate continental monsoon climates with a long and cold winter. The terrain is generally high in the northwest, north, and southeast and low in the northeast and southwest. Its topography consists of mountains, mesas, plains, and water bodies. The average annual snowfall was 31 mm from 1961 to 2015, with a maximum of 71 mm [64]. Yichun City is located in the Xiaoxing'anling Mountains. Eighty percent of the local terrain is mountainous, and 5% is water, 5% is grassland, and 10% is field. Overall, the terrain is high in the northwest and low in the southeast. The terrain is steep in the south, gentle in the middle, and flat in the north. The average altitude is 600 m. It has a mid-temperate continental humid monsoon climate. The climate is cold and dry and is controlled by the polar continental air mass in winter. It is affected by the subtropical marine air mass in summer, and the precipitation is concentrated in this season. With abundant rainfall and a long sunshine duration, the climate is hot and humid and is suitable for crop growth (despite occasional cold damage). During spring and autumn, the weather can vary. The spring is windy with little precipitation and is prone to droughts. The autumn is characterized by rapid cooling, frequent dry frosts, and cold damage. The annual average temperature is 0.6 °C, the annual precipitation is 610.5 mm, and the annual sunshine duration is 2196.0 h. Dark brown soil is the main soil type in Heilongjiang Province, and the soil in Yichun City is also predominantly dark brown soil. Therefore, an experimental site with dark brown soil was selected (Figure 1).

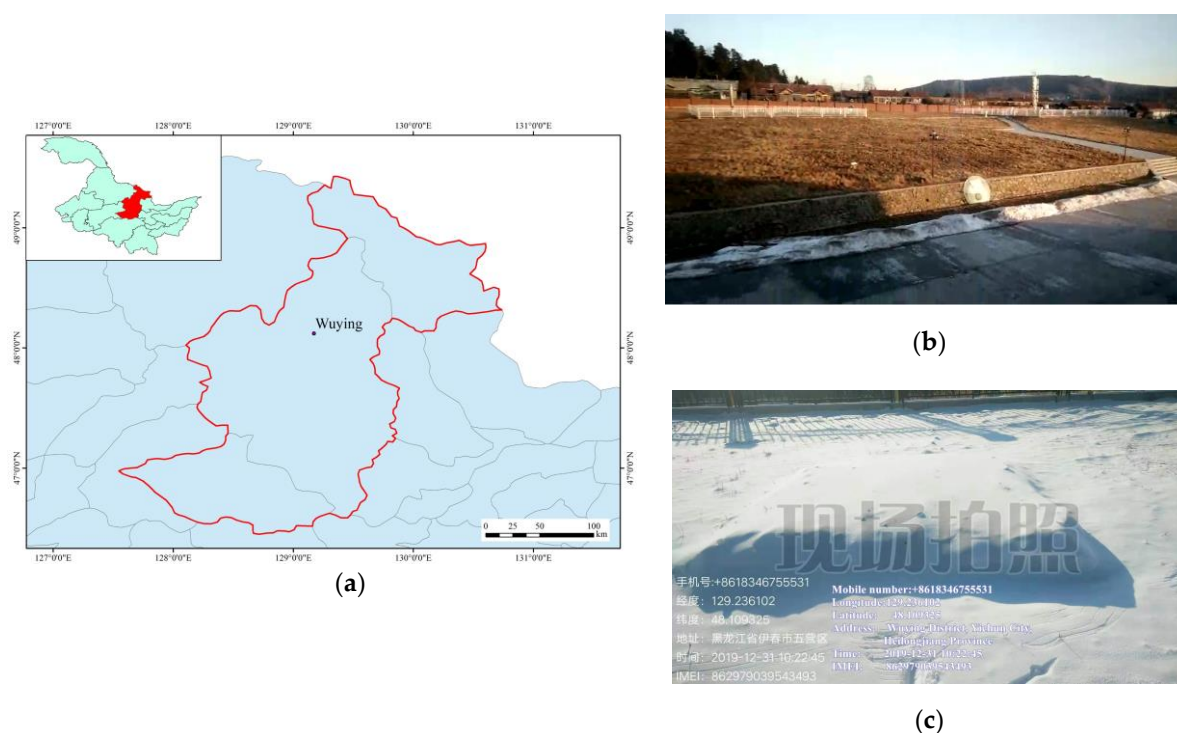


**Figure 1.** The test area. (a) The location of experiment quadrats; (b) The quadrats before experiment; (c) The quadrats during experiment.

### 2.2. Meteorological Conditions during the Experimental Period

The trial was conducted from October 2019 to June 2020. After the snowfall in November 2019, the snowpack test was completed, and the sampling was from March to June 2020. The temperature and precipitation on the precipitation days at Wuying Station during the sampling period are shown in Figure 2. According to the observation records, a total of

24 precipitation events occurred during the sampling period, of which the first four were snowfall, the fifth (17 April 2020) was sleet, and the other 19 were rainfall events. The highest precipitation occurred on 27 May, with a rainfall of 45.5 mm; and the lowest rainfall events (0.1) mm occurred on 26 March, 17 April, and 22 April. The first snowfall event recorded during the experiment occurred on March 12, when 10 cm of snow had melted (11 March). Thus, except for this snow day, the average temperature on all of the other days was above 0 °C. The highest temperature was 17.6 °C on 13 May, and the lowest temperature was −6.9 °C on 13 March.

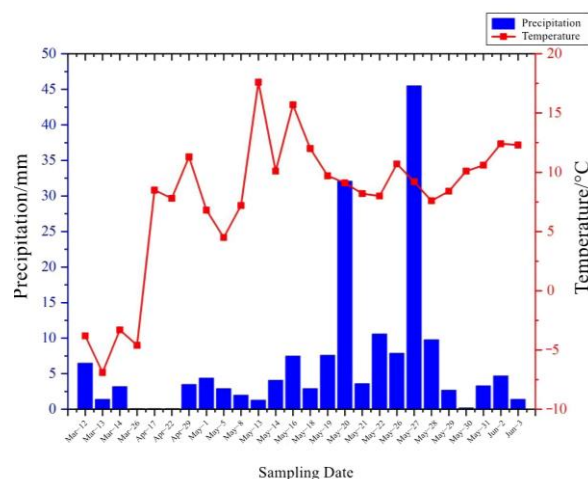


**Figure 2.** The change of temperature and precipitation amount in Wuying during the time of the experiment.

### 2.3. Experimental Design

**Design of the experimental site:** The experimental quadrat was designed as a square, with each side measuring 3 m. After the first snow cover of 30 cm, the method of manual removal and filling was used to control the three quadrats with snow thicknesses of 10 cm, 30 cm, and 50 cm. The same method was used to make three replicas for each snow depth. Three quadrats without snow cover in the same area were prepared as control quadrats. If there was any new snowfall throughout the winter, plastic was used to keep the snow from falling on these experimental plots. However, if there was a decrease in the snow thickness, snow was added to maintain the snow thickness in the plots with snow. To facilitate sampling and exclude the influence of the surrounding snow on the snow in the quadrats, as well as the influence of the surrounding snowmelt water on the soil, a 50 cm plastic diaphragm was vertically buried around each quadrat in advance, and a one-meter-wide access was left around the quadrat (Table 1).

**Sampling:** Before the snow began to melt, soil samples were collected from three depth intervals (0–10 cm, 10–20 cm, and 20–30 cm) using a soil drill. These samples were used as a baseline to measure the initial isotope values of the soil water. After the snow had completely melted in each experimental quadrat, soil samples were collected from the three depth intervals (0–10 cm, 10–20 cm, and 20–30 cm) using a soil drill. Soil samples were acquired every three days. The soil samples were stored in whirl-pak sterile sampling bags, sealed, and stored in a refrigerator. A total of 243 soil samples were collected. In addition, snow samples were collected from the 10 cm, 30 cm, and 50 cm quadrats before the snow melted. These samples were stored in whirl-pak sterile sampling bags, sealed, and stored in a refrigerator. During the experiment, a sample of each precipitation event was collected using a J10622 rain gauge. After each collection, the sample was stored in a sterile water sample bag, sealed, and stored in a refrigerator. The samples were transferred to the Harbin Normal University for laboratory analysis.

**Table 1.** The diagram of the experiment.

	Contents	Equipment
Experiment time	November 2019–June 2020	
Experiment area	Four sample plots were selected and subjected to four treatments of bare ground, snow thickness 10 cm, snow thickness 30 cm, and snow thickness 50 cm, and repeated three times. A 50 cm plastic membrane was embedded vertically around each test plot, and a one-meter-wide passage was left around the plot.	Artificially piled up
Sampling depth of soil	0–10 cm, 10–20 cm, 20–30 cm	Earth drill
Sampling time	Once every three days after the snow cover had totally melted on every plot	-
Sampling method	The soil samples taken out were stored in whirl-pak sterile sampling bags, sealed and stored in the refrigerator. A total of 243 soil samples were collected. We used the J10622 rain gauge to collect each precipitation sample, put it into a sterile water sample bag after each collection, sealed it and stored it in the refrigerator. We collected snow samples, store them in whirl-pak sterile sampling bags, sealed them, and stored them in the refrigerator.	-
Sample preprocessing	Treatment of soil samples: The soil samples were subjected to vacuum condensation water extraction with a vacuum distillation device. The extracted soil water was filtered through a 0.45 $\mu\text{m}$ organic filter membrane and placed in a 2 mL injection bottle for storage in a sealed and refrigerated manner. Treatment of snow samples and precipitation samples: The snow melt water and precipitation were filtered with a 0.45 $\mu\text{m}$ organic filter membrane, and then placed in a 2 mL injection bottle, sealed and refrigerated.	-
Isotope determination	Needle washing of sample, reduction reaction in elemental analyzer EA, mass spectrometer to measure and compare	-

**Sampling:** Before the snow began to melt, soil samples were collected from three depth intervals (0–10 cm, 10–20 cm, and 20–30 cm) using a soil drill. These samples were used as a baseline to measure the initial isotope values of the soil water. After the snow had completely melted in each experimental quadrat, soil samples were collected from the three depth intervals (0–10 cm, 10–20 cm, and 20–30 cm) using a soil drill. Soil samples were acquired every other day. The soil samples were stored in whirl-pak sterile sampling bags, sealed, and stored in a refrigerator. A total of 243 soil samples were collected. In addition, snow samples were collected from the 10 cm, 30 cm, and 50 cm quadrats before the snow melted. These samples were stored in whirl-pak sterile sampling bags, sealed, and stored in a refrigerator. During the experiment, a sample of each precipitation event was collected using a J10622 rain gauge. After each collection, the sample was stored in a sterile water sample bag, sealed, and stored in a refrigerator. The samples were transferred to the Harbin Normal University for laboratory analysis.

According to the experimental records, the snow began to melt on 2 March, and the snow depth gradually decreased. When the snow depth was 0 cm, the first soil sample was collected. On 8 March, the 10 cm snow depth had completely melted. Due to the low temperature, the snowmelt water could not infiltrate into the deep soil. For the purposes of our experiment, only the 0–10 cm soil layer samples were collected, and samples were also collected at the corresponding soil depth from the control plots. On 11 March, the 30 cm snow depth plots had completely melted, and on 18 March, the 50 cm snow depth had completely melted. On the day when each snow depth plot melted, 0–10 cm soil samples were taken from the plots with different snow depths. From 8 April onward, soil samples were collected at depths of 0–10 cm and 10–20 cm; and from April 14 onward, soil samples

were collected at depths of 0–10 cm, 10–20 cm, and 20–30 cm. These samples were collected every three days. Soil samples were brought back to the laboratory for water extraction using a two-hour vacuum extraction process, and the average value was measured three times using a MAT-253 stable isotope ratio mass spectrometer.

#### 2.4. Determination of Hydrogen and Oxygen Isotopes

##### 2.4.1. Isotope Calculation Method and Measurement Standard

Stable isotopes make up the majority of Earth (for example  $^{12}\text{C}$ ,  $^{16}\text{O}$ ), and some of them are not abundant, such as the content of hydrogen and oxygen isotopes referred to in this paper. Therefore, in practice, the relative measurement method is often used to compare the ratio of a heavy isotope to a light isotope in the sample to be tested (Sa)  $R_{Sa}$  with the ratio of a standard material (St)  $R_{St}$ . The comparison result is called the  $\delta$  value of the sample, i.e., the difference between the isotope ratio of the sample and the isotope ratio of the standard material. The calculation formula is

$$\delta = \left( \frac{R_{Sa}}{R_{St}} - 1 \right) \times 1000 \frac{0}{00} \quad (1)$$

The  $\delta$  value is related to the standard material used. Thus, it is necessary to select a suitable standard material for isotopic analysis, and in the comparison of different samples, the same measurement standard must be used to yield a reliable result. In this study, the international standard sample, the Vienna Standard Mean Ocean Water (VSMOW), was selected as the standard; and its hydrogen and oxygen isotope values are  $\delta\text{D}_{\text{VSMOW}} = 0\text{‰}$  and  $\delta^{18}\text{O}_{\text{VSMOW}} = 0\text{‰}$ , respectively.

##### 2.4.2. Sample Treatment and Analysis

(1) Preparation of soil samples (left picture in Figure 3): After samples were transported to the laboratory, it was necessary to pretreat the soil samples. A vacuum extraction device was used to perform the vacuum condensation and water extraction from the collected soils. The extracted water was filtered through a  $0.45 \mu\text{m}$  organic filter membrane, placed in a 2 mL injection bottle, sealed, and refrigerated.



**Figure 3.** The pictures in the experiment process. (a) Moisture extraction equipment; (b) Isotope analysis equipment.

(2) Preparation of snow samples and precipitation samples: The snowmelt water and precipitation samples were filtered through a  $0.45 \mu\text{m}$  organic filter membrane, placed in a 2 mL injection bottle, sealed, and refrigerated.

(3) Isotope analysis: The sample was placed on the automatic sampling tray, and the automatic liquid sampler washed the needle in the sample three times according to the set procedure. On the fourth time,  $0.1 \mu\text{L}$  of sample was extracted, and the sample was reduced in the elemental analyzer to produce  $\text{H}_2$  and  $\text{CO}$ . After completing the reduction

reaction, a mixture of gases (of the reference gas ( $H_2$  and  $CO$  in the cylinder), the  $H_2$  and  $CO$  was generated, and the carrier gas (high-purity helium)) was introduced into the mass spectrometer through the ConFlo-IV Universal Interface. The mass spectrometer measured and calculated the  $\delta D$  and  $\delta^{18}O$  values. The obtained  $\delta D$  and  $\delta^{18}O$  values were determined relative to VSMOW. During sample analysis, the test spectrum and real-time data were monitored to ensure normal and stable operation of the instrument. The instruments and equipment used are shown in Figure 3b. The instrument error was 1‰ (H), 0.4‰ (O).

### 2.5. Binary Mixing Model

In this study, the isotope binary mixing model was used to calculate the contribution of the snowmelt water to the soil water. The calculation formulas are as follows:

$$\begin{cases} f_1 \times \delta D_1 + f_2 \times \delta D_2 = \delta D \\ f_1 + f_2 = 1 \end{cases} \quad (2)$$

and

$$\begin{cases} f_1 \times \delta^{18}O_1 + f_2 \times \delta^{18}O_2 = \delta^{18}O \\ f_1 + f_2 = 1 \end{cases} \quad (3)$$

$\delta D$  and  $\delta^{18}O$  are the integrated isotope values;  $\delta D_1$  and  $\delta D_2$  (for H) and  $\delta^{18}O_1$  and  $\delta^{18}O_2$  (for O) are the water isotope values of the different sources, such as the different soil layers or different water sources; and  $f_1$  and  $f_2$  are the proportions of the different sources, that is, the contributions of the different sources to the integrated results.

#### Calculation Example

(1) Contribution of the snowmelt water to soil water before precipitation. We take the 0–10 cm soil depth interval with a 10 cm snow depth on 8 March as an example. It is known that before the snow melted, the hydrogen and oxygen isotopes of the snow were  $\delta D = -76.62\text{‰}$  and  $\delta^{18}O = -23.54\text{‰}$ , respectively; the hydrogen and oxygen isotopes of the 0–10 cm soil water were  $\delta D = -128.44\text{‰}$  and  $\delta^{18}O = -16.67\text{‰}$ , respectively; and the hydrogen and oxygen isotopes of the 0–10 cm soil water were  $\delta D = -39.92\text{‰}$  and  $\delta^{18}O = -17.43\text{‰}$ , respectively. Assuming that the contribution of the original soil water to the soil water after the snow melted is  $x_1$ , and the contribution of the snowmelt water to the soil water after the snow melted is  $x_2$ , the simultaneous equations for the hydrogen isotopes are as follows:

$$\begin{cases} 128.44x_1 + 76.62x_2 = 39.92 \\ x_1 + x_2 = 1 \end{cases} \quad (4)$$

By solving these equations, we obtained  $x_1 = 0.7617$ ,  $x_2 = 0.2383$ . Thus, the contribution of snowmelt water to soil water was 23.83%.

Similarly, we can establish the simultaneous equations for the oxygen isotopes:

$$\begin{cases} 16.67x_1 + 23.54x_2 = 17.43 \\ x_1 + x_2 = 1 \end{cases} \quad (5)$$

By solving these equations, we obtained  $x_1 = 0.8773$ ,  $x_2 = 0.1227$ . That is, the contribution of snowmelt water to soil water was 12.27%.

In summary, the contribution of snowmelt water to soil water on 8 March was 12.27–23.83%, with an average of 18.05%.

(2) Contribution of snowmelt water to soil water after precipitation. The calculation method for the contribution of the snowmelt water to the soil water after precipitation uses the hydrogen and oxygen isotopes of soil water before precipitation and the precipitation hydrogen and oxygen isotopes to obtain the soil water isotope value after precipitation. After removing the influence of the precipitation, the upper and lower limits of the contribution value can be obtained by multiplying the change in the soil itself by the contribution value. We take the soil layer depth interval of 10 cm with a 10 cm snow depth on 18 March as an example. It is known that the hydrogen and oxygen isotopes of the soil before the

precipitation were  $\delta D = -124.63\text{‰}$  and  $\delta^{18}\text{O} = -15.35\text{‰}$ , respectively; the hydrogen and oxygen isotopes of the precipitation were  $\delta D = -136.43$  and  $\delta^{18}\text{O} = -18.59\text{‰}$ , respectively; and the hydrogen and oxygen isotopes of the 0–10 cm soil interval after the precipitation were  $\delta D = -128.38\text{‰}$  and  $\delta^{18}\text{O} = -15.50\text{‰}$ , respectively. We assume that the contribution of the soil water before the precipitation to the soil water after the precipitation is  $x_1$ , and the contribution of the precipitation to soil water after precipitation is  $x_2$ . The simultaneous equations for the hydrogen isotopes are as follows:

$$\begin{cases} 124.63x_1 + 136.43x_2 = 128.38 \\ x_1 + x_2 = 1 \end{cases} \quad (6)$$

By solving these equations, we obtained  $x_1 = 0.6819$ ,  $x_2 = 0.3181$ . That is, the contribution of the original soil water to the soil water after precipitation was 68.19%.

Similarly, the simultaneous equations for the oxygen isotopes are as follows:

$$\begin{cases} 15.35x_1 + 18.59x_2 = 15.50 \\ x_1 + x_2 = 1 \end{cases} \quad (7)$$

By solving these equations, we obtained  $x_1 = 0.9528$ ,  $x_2 = 0.0472$ , i.e., the contribution of the original soil water to the soil water after precipitation was 95.28%.

According to Equation (4), the contribution of the snowmelt water based on the hydrogen isotopes of the original soil water was 23.83%. Therefore, after the precipitation on 18 March, the contribution of the snowmelt water to the soil water calculated based on the hydrogen isotopes was  $0.6819 \times 0.2383 = 0.1625$ . The contribution of the snowmelt water calculated based on the oxygen isotopes was 12.27%. Thus, after the precipitation on 18 March, the contribution of the snowmelt water to the soil water calculated based on the oxygen isotopes was  $0.9528 \times 0.1227 = 0.1169$ . In summary, the contribution of the snowmelt water to the soil water on March 18 after the precipitation was 11.69–16.25%, with an average of 13.97%. The calculation method for the contribution range of the snowmelt water on other days is the same as the example provided above.

### 3. Results

#### 3.1. Distribution Characteristics of Isotopes of Snowmelt Water, Soil Water, and Precipitation

The hydrogen and oxygen isotopes of snowmelt water and soil water are presented in Table 2. The oxygen isotope values for the 10 cm, 30 cm, and 50 cm snow depth plots are quite similar. However, their deuterium values fluctuate more widely than their oxygen isotope values. For the snow depths of, 10 cm, 30 cm, and 50 cm, the deuterium values were  $-176.62\text{‰}$ ,  $-169.99\text{‰}$ , and  $-172.61\text{‰}$ , respectively; and the oxygen isotope values were  $-23.54\text{‰}$ ,  $-23.77\text{‰}$ , and  $-24.15\text{‰}$ , respectively. For the soil depth intervals of 0–10 cm, 10–20 cm, and 20–30 cm, the deuterium values were  $-128.44\text{‰}$ ,  $-99.22\text{‰}$ , and  $-94.40\text{‰}$ , respectively; and the oxygen isotope values were  $-16.57\text{‰}$ ,  $-12.49\text{‰}$ , and  $-11.43\text{‰}$ , respectively. With an average of 13.97%, the standard deviation is 3.22%. The standard deviation is more than 10% of the original value, indicating that the change is less stable. It can be seen that with the increase of soil depth, the hydrogen and oxygen isotope values show a gradual increase. It shows that with the increase of soil depth, the isotopes in the bare soil water before melting snow gradually enrich, and the hydrogen and oxygen isotopes have a good consistency change. It is consistent with the change law of hydrogen and oxygen isotopes.

The hydrogen and oxygen isotope values fluctuated greatly in previous precipitation events. The hydrogen isotope values fluctuated between  $-176.91\text{‰}$  and  $-24.79\text{‰}$ , with an average of  $-90.62\text{‰}$ ; and the oxygen isotope values fluctuated between  $-23.97\text{‰}$  and  $-3.30\text{‰}$ , with an average of  $-12.50\text{‰}$ . The hydrogen isotope values of the snowfall were generally low, fluctuating between  $-176.91\text{‰}$  and  $-161.99\text{‰}$ , with an average of  $-146.55\text{‰}$ ; while the hydrogen isotope values of the rainfall were mostly concentrated above  $-100\text{‰}$ , with an average of  $-79.97\text{‰}$ . The oxygen isotope values of the snowfall

ranged between  $-23.61\text{‰}$  and  $-21.79\text{‰}$ , with an average of  $-19.39\text{‰}$ . The oxygen isotope values of the rainfall were mostly concentrated above  $-15\text{‰}$ , with an average of  $-11.14\text{‰}$ . These value ranges reflect the influence of the precipitation in the different phases on the isotope values.

**Table 2.** The characteristics of the isotopes of the different types of water before the snow melted ( $\text{‰}$ ).

Isotope	Snowmelt Water			Soil Water			Precipitation	
	10 cm	30 cm	50 cm	0–10 cm	10–20 cm	20–30 cm	Average Rainfall	Average Snowfall
$\delta\text{D}$	−176.62	−169.99	−172.61	−128.44	−99.22	−94.40	−79.97‰	−146.55‰
$\delta^{18}\text{O}$	−23.54	−23.77	−24.15	−16.57	−12.49	−11.43	−11.14‰	−19.39‰

### 3.2. Distribution Characteristics of Isotopes of Soil under Different Snow Depths

Table 3 shows the distribution of the soil water's isotopes in the 0 cm, 10 cm, 30 cm, and 50 cm snow depth plots at different soil depths. From the average distribution, in the 0 cm, 10 cm, 30 cm, and 50 cm snow cover plots and the 0–30 cm soil layer, the  $\delta\text{D}$  contents were  $-82.12\text{‰}$ ,  $-88.18\text{‰}$ ,  $-88.38\text{‰}$ , and  $-87.69\text{‰}$ , respectively; and the  $\delta^{18}\text{O}$  contents were  $-9.89\text{‰}$ ,  $-11.12\text{‰}$ ,  $-11.34\text{‰}$ , and  $-11.20\text{‰}$ , respectively. Large fluctuations occurred in the 0–10 cm soil layer; while in the 10–20 cm and 20–30 cm layers, the  $\delta\text{D}$  and  $\delta^{18}\text{O}$  values basically increased with increasing snow depth.

**Table 3.** Distribution of the isotope values of the soil for different snow depths ( $\text{‰}$ ).

Snow Depth	Isotope	0–10 cm	10–20 cm	20–30 cm	Average
Bare land	$\delta\text{D}$	−92.93	−79.28	−74.14	−82.12
	$\delta^{18}\text{O}$	−10.66	−9.77	−9.25	−9.89
10 cm	$\delta\text{D}$	−102.69	−83.22	−78.64	−88.18
	$\delta^{18}\text{O}$	−12.57	−10.60	−10.20	−11.12
30 cm	$\delta\text{D}$	−99.54	−85.71	−79.88	−88.38
	$\delta^{18}\text{O}$	−12.51	−11.03	−10.48	−11.34
50 cm	$\delta\text{D}$	−96.04	−86.28	−80.75	−87.69
	$\delta^{18}\text{O}$	−11.95	−11.10	−10.54	−11.20

Figures 4–6 show the changes in the soil water's isotopes in the 0 cm, 10 cm, 30 cm, and 50 cm snow depth plots at different soil depths. Overall, the changes in the isotopes of the soil water under different snow depths with time were quite consistent. Specifically, for the soil under each snow depth, the  $\delta\text{D}$  and  $\delta^{18}\text{O}$  values gradually increased with time. After reaching a peak in the later period, they decreased rapidly. For the different snow depths, the  $\delta\text{D}$  and  $\delta^{18}\text{O}$  values of the different soil layers exhibited similar characteristics. Significant fluctuations occurred in the 0–10 cm soil layer, while the fluctuations in the 10–20 cm and 20–30 cm layers were relatively small, indicating that the strong influence of precipitation was limited to the soil water in the surface layer since the soil layers below 10 cm were not directly in contact with the atmosphere. This influence was weakened by the upper soil layer, and the deeper layers were relatively stable.

Variance analysis was used to further analyze the differences in the isotope values of each soil layer, and the results are presented in Tables 4 and 5. Table 4 shows that for the different snow depth and the same soil layer, the soil water's isotope values of the 50 cm snow depth plot and the other snow depth plots were significantly different ( $p < 0.05$ ), and there was no significant difference between the other three snow depth plots (0, 10, and 30 cm). For the different snow depths, the soil water's isotope values in the 0–10 cm soil layer were greatly affected by precipitation. As the snowmelt completion time increased, the difference between the soil water's isotopes and the atmospheric precipitation's isotopes gradually decreased. However, as the soil depth increased, the influence of the atmospheric precipitation on the soil water's isotopes was weakened or delayed. The distributions and

trends of the deuterium and oxygen isotopes were highly consistent. Table 5 shows that there was a significant difference between the 20–30 cm layer and the other two layers ( $p < 0.05$ ); while there was no difference in the soil water’s isotope values between the 0–10 cm and 10–20 cm layers.

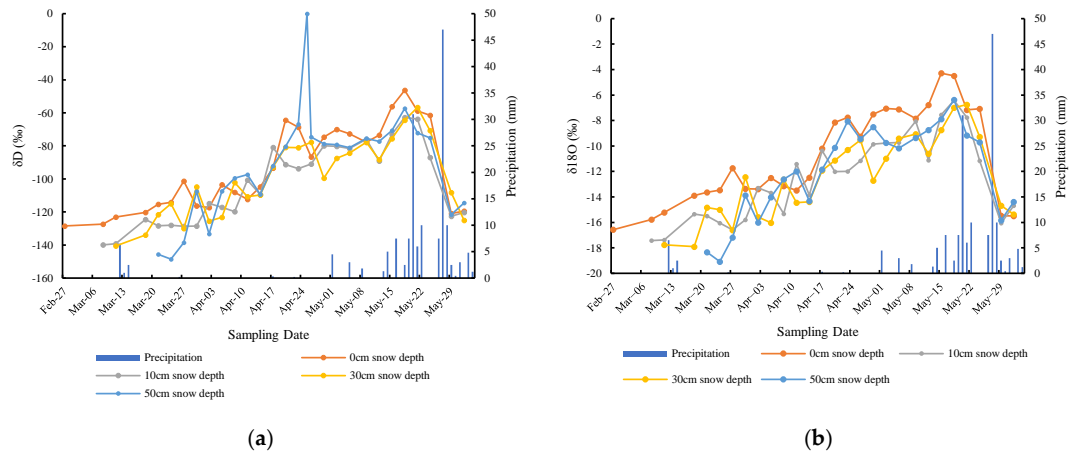


**Figure 4.** The change with time of  $\delta D$  and  $\delta^{18}O$  in soil water of different snow depth in 0–10 cm soil depth. (a) The change of  $\delta D$  (b) The change of  $\delta^{18}O$ .

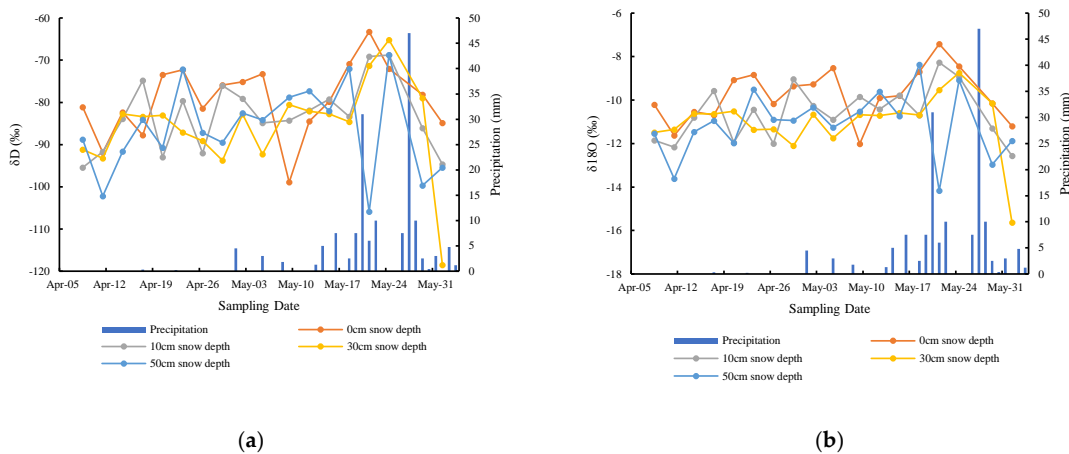


**Figure 5.** The change with time of  $\delta D$  and  $\delta^{18}O$  in soil water of different snow depth in 10–20 cm soil depth. (a) The change of  $\delta D$  (b) The change of  $\delta^{18}O$ .

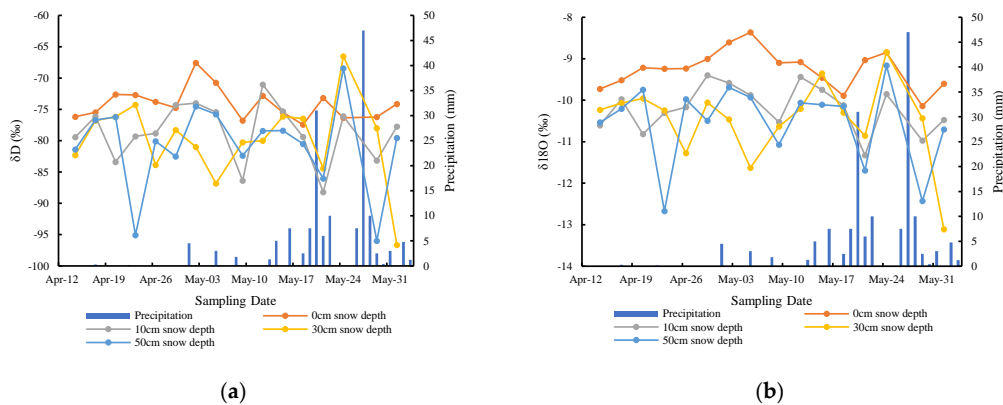


**Figure 6.** The change with time of  $\delta D$  and  $\delta^{18}O$  in soil water of different snow depth in 20–30 cm soil depth. (a) The change of  $\delta D$  (b) The change of  $\delta^{18}O$ .

**Table 4.** Differences in the isotope values of the soil water in the same soil layer for different snow depths.

Snow Cover \ Soil Layer	$\alpha = 0.05$			$\alpha = 0.01$		
	0–10 cm	10–20 cm	20–30 cm	0–10 cm	10–20 cm	20–30 cm
0 cm	−10.66 <sup>a</sup>	−9.77 <sup>a</sup>	−9.25 <sup>a</sup>	−10.66 <sup>A</sup>	−9.77 <sup>A</sup>	−9.25 <sup>A</sup>
10 cm	−12.57 <sup>a</sup>	−10.60 <sup>a</sup>	−10.20 <sup>a</sup>	−12.57 <sup>A</sup>	−10.60 <sup>A</sup>	−10.20 <sup>A</sup>
30 cm	−12.51 <sup>a</sup>	−11.03 <sup>a</sup>	−10.48 <sup>a</sup>	−12.51 <sup>A</sup>	−11.03 <sup>A</sup>	−10.48 <sup>A</sup>
50 cm	−11.95 <sup>b</sup>	−11.10 <sup>b</sup>	−10.54 <sup>b</sup>	−11.95 <sup>A</sup>	−11.10 <sup>A</sup>	−10.54 <sup>A</sup>

Letters represent differences between groups. With the same letter represent no difference between groups, otherwise, there is a difference.

**Table 5.** Differences in the isotope values of the soil water in the different soil layers for the same depth.

Soil Layer \ Snow Cover	$\alpha = 0.05$			$\alpha = 0.01$		
	10 cm	30 cm	50 cm	10 cm	30 cm	50 cm
0–10 cm	−12.57 <sup>a</sup>	−12.51 <sup>a</sup>	−11.95 <sup>a</sup>	−12.57 <sup>A</sup>	−12.51 <sup>A</sup>	−11.95 <sup>A</sup>
10–20 cm	−10.60 <sup>a</sup>	−11.03 <sup>a</sup>	−11.10 <sup>a</sup>	−10.60 <sup>A</sup>	−11.03 <sup>A</sup>	−11.10 <sup>A</sup>
20–30 cm	−10.20 <sup>b</sup>	−10.48 <sup>b</sup>	−10.54 <sup>b</sup>	−10.20 <sup>A</sup>	−10.48 <sup>A</sup>	−10.54 <sup>A</sup>

Letters represent differences between groups. With the same letter represent no difference between groups, otherwise, there is a difference.

### 3.3. Characteristics of the Contributions of Snow Cover to Soil Water

#### 3.3.1. Distribution Characteristics of Contributions of Different Snow Depths to Soil Water

Results (Table 6) show that the different snow depths contributed to the soil moisture at soil depths of 0–30 cm. On average, the contributions of the 10 cm, 30 cm, and 50 cm snow depths to the soil moisture were 8.13%, 8.55%, and 11.24%, respectively, i.e., the greater the snow depth, the greater the contribution to the soil moisture. The contributions of the 10 cm, 30 cm, and 50 cm snow depths to the soil moisture in the different soil layers were also different, i.e., the greater the snow depth, the greater the contribution. Taking the 0–10 cm soil layer as an example, the contributions of the 10 cm, 30 cm, and 50 cm snow depths were 9.14%, 9.25%, and 15.87%, respectively. The same characteristics were also found for the 10–20 cm and 20–30 cm soil layers.

#### 3.3.2. Change Characteristics of Contributions of Different Snow Depths to Soil Water

Figure 7 shows the curves of the contributions of the snow depths to the different soil layers with time. The retention times of the contributions of the different snow depths in the 0–30 cm soil layer were basically the same, and the retention times of the contributions of the 10 cm, 30 cm, and 50 cm snow depths in the 0–30 cm soil layer were 61 d, 62 d, and 62 d, respectively. Nevertheless, the retention times of the contributions of the different snow depths in the different soil layers were inconsistent. The retention time in the 0–10 cm soil layer was the longest (average of 69 d), followed by that in the 20–30 cm soil layer (average of 59 d), and that in the 10–20 cm soil layer was the shortest (average of 54 d).

**Table 6.** Contributions (%) and their retention times(d) of the different snow depths to the soil water.

Snow Cover \ Soil Layer	0–10 cm		10–20 cm		20–30 cm	
	Duration	Contribution	Duration	Contribution	Duration	Contribution
10 cm	71	9.14	51	8.82	67	6.43
30 cm	71	9.25	55	9.23	62	7.17
50 cm	64	15.87	55	10.32	48	7.53
Average	69	11.42	54	9.46	59	7.04

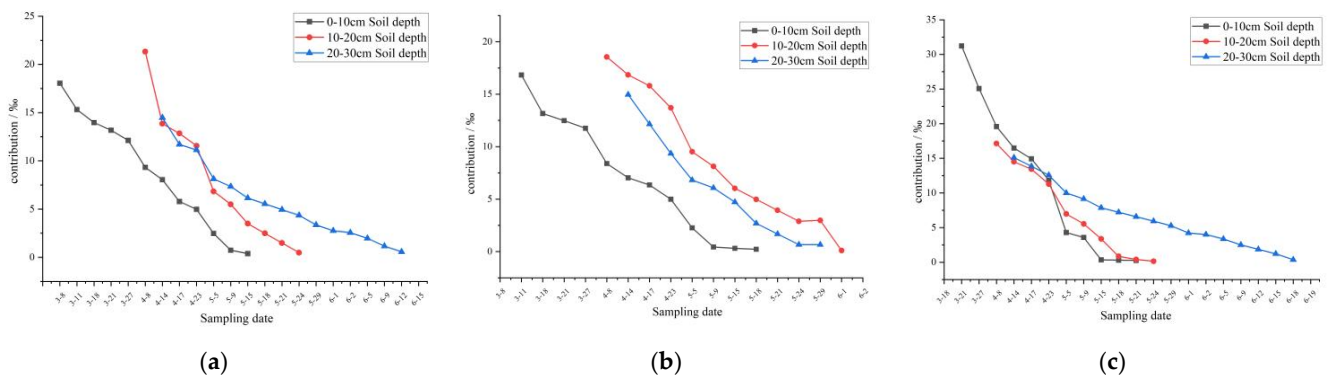


**Figure 7.** Contribution of snowmelt water to soil water at 10 cm soil layer (a), 30 cm soil layer (b), 50 cm soil layer (c).

Figure 7 shows that the contributions of the different snow depths to the different soil layers exhibited a nearly linear trend with time (equations are shown in Table 7). The water contributions of the different snow depths in the different soil layers decreased significantly with time, and their rates of decrease did not exhibit obvious regularity. For the 0–10 cm, 10–20 cm, and 20–30 cm soil layers, the average contributions of the snow to the soil water were  $-0.33\%/d$ ,  $-0.37\%/d$ , and  $-0.26\%/d$ , respectively.

**Table 7.** Simulation equation of the dynamic process of the contribution of the snow depth to the soil water in the different soil layers.

Soil Layer	Snow Cover			
	0–10 cm	10–20 cm	20–30 cm	
10 cm	$y = -0.251x + 16.803$ ** $R^2 = 0.995$	$y = -0.392x + 17.952$ ** $R^2 = 0.961$	$y = -0.213x + 13.028$ ** $R^2 = 0.987$	
30 cm	$y = -0.233x + 15.064$ ** $R^2 = 0.994$	$y = -0.346x + 18.817$ ** $R^2 = 1.00$	$y = -0.306x + 13.468$ ** $R^2 = 0.982$	
50 cm	$y = -0.505x + 29.022$ ** $R^2 = 0.994$	$y = -0.346x + 18.817$ ** $R^2 = 0.995$	$y = -0.217x + 14.660$ ** $R^2 = 0.999$	

\*\* means significance at 0.01 levels.

The dynamic distribution of the contributions and the variance analysis are presented in Table 8. The results indicate that the contributions of the different snow depths to the soil water in a given soil layer were significantly different. Specifically, the contributions of the 10 cm and 30 cm snowmelt water to the 0–10 cm soil layer were not significantly different, whereas the contribution of the 50 cm snowmelt water was significantly larger than that of the 10 cm and 30 cm snowmelt water. For the 10–20 cm and 20–30 cm soil layers, the contributions of the 10 cm, 30 cm, and 50 cm snowmelt water were significantly different, indicating that the water content of the deep soil was more sensitive to the snow depth. Table 8 also shows that for the same snow depth, the contributions to the different soil layers were also significantly different. Specifically, the contribution of the 10 cm snowmelt water to the 0–10 cm soil layer was significantly different than those to the 10–20 cm and 20–30 cm soil layers; while the contributions to the 10–20 cm and 20–30 cm soil layers were not significantly different. The contributions of the 30 cm and 50 cm snow depths to the 0–10 cm, 10–20 cm, and 20–30 cm soil layers were significantly different. That is, when the snow depth reached a certain depth, the contributions to the different depth soil layers were different, and the contribution increased with increasing soil depth.

**Table 8.** Analysis of variance of the contribution of the snow cover to the soil water ( $\alpha = 0.05$ ).

Snow Cover \ Soil Layer	Soil Layer			Snow Cover			
	0–10 cm	10–20 cm	20–30 cm	10 cm	20 cm	30 cm	
10 cm	7.932 <sup>a</sup>	7.156 <sup>a</sup>	5.973 <sup>a</sup>	0–10 cm	7.932 <sup>a</sup>	6.374 <sup>a</sup>	10.309 <sup>a</sup>
30 cm	6.374 <sup>a</sup>	7.794 <sup>b</sup>	5.303 <sup>b</sup>	10–20 cm	7.156 <sup>b</sup>	7.794 <sup>b</sup>	6.548 <sup>b</sup>
50 cm	10.309 <sup>b</sup>	6.548 <sup>c</sup>	7.014 <sup>c</sup>	20–30 cm	5.973 <sup>b</sup>	5.303 <sup>c</sup>	7.014 <sup>c</sup>

Letters represent differences between groups. With the same letter represent no difference between groups, otherwise, there is a difference.

### 3.4. Simulation of the Contributions of Snowmelt Water and Precipitation to Soil Moisture

The contribution of the snowmelt water to the soil water is affected by the snow depth and precipitation. To reveal the general pattern of the contributions of the snow depth and precipitation to the soil water, a relationship between the three was determined. By taking the soil layer's depth and the average snowmelt water contribution to the three layers under each snow depth as  $y$ , the snow depth as  $x_1$  and the precipitation as  $x_2$ , multiple regression equations were formulated. The standardized coefficients of the equations are listed in Table 9.

**Table 9.** Standardized coefficients of contribution equation for each soil layer.

Soil Layer	$x_1$	$x_2$	$R^2$
0–10 cm	0.331	−0.702	0.461 **
10–20 cm	0.106	−0.751	0.596 **
20–30 cm	0.201	−0.801	0.661 **
Three-layer average	0.148	−0.656	0.435 **

\*\* means significance at 0.01 levels.

The above equations passed the significance test ( $p < 0.01$ ). According to the equations, for the 0–10 cm soil layer, the contribution of the precipitation to the soil water decreased by about 0.702% for every 1 mm increase in precipitation, while the contribution of the snowmelt water to the soil water increased by about 0.331% for every 1 mm increase in snow depth. For the 10–20 cm soil layer, the contribution of the precipitation to the soil water decreased by 0.751% for every 1 mm increase in precipitation, while the contribution of the snowmelt water to the soil water increased by 0.106% for every 1 mm increase in the snow depth. For the 20–30 cm soil layer, the contribution of the precipitation to the soil water decreased by 0.801% for every 1 mm increase in precipitation, while the contribution of the snowmelt water to the soil water increased by 0.201% for every 1 mm increase in the snow depth. For the average depths of the three soil layers, the contribution of the precipitation to the soil water decreased by 0.656% for every 1 mm increase in precipitation, while the contribution of the snowmelt water to the soil water increased by 0.148% for every 1 mm increase in the snow depth.

## 4. Discussion

(1) In this study, outdoor experiments were conducted on the typical soil type in northeastern China, and the influence of the snow cover on the soil water content was investigated. Using the unique advantages of hydrogen and oxygen isotopes, the contribution of the snowmelt water to the surface soil water in the spring and its dynamic changes were quantitatively analyzed. The results offer guidance for preventing the adverse effects of spring droughts on agricultural production and provide a scientific basis and information for agricultural irrigation and agricultural water resource allocation.

(2) For some test results in this paper, compare them with the existing research. From July 2000 to May 2001, Robertson et al. selected two sampling sites in Cle Elum and Ellensburg with different precipitations on the eastern slope of the Cascade Mountains in Washington State, and analyzed the seasonal variation of oxygen isotopes in soil water. Among them, the annual precipitation of the Cle Elum sampling point is 564 mm, which

is similar to the annual precipitation of 610.5 mm in the study area of this paper [52]. The study found that the oxygen isotope in the 10 cm soil of Cle Elum during the spring snow melting was  $-10.775$ , and in this paper it was  $-10.868$ , which means they are basically the same. The difference lies in the soil texture and ambient temperature. Cle Elum is sandy loam soil, and the soil in this study area is dark brown soil; the annual average temperature of Cle Elum is  $8.1\text{ }^{\circ}\text{C}$ , and the annual average temperature of this study area is  $0.6\text{ }^{\circ}\text{C}$ . Therefore, regarding the influence of different soil textures and environments on soil isotope content and changes, it remains to be further explored in the future to obtain a more accurate and widely credible law. At the same time, it also reminds us that expanding the spatial scale of the study, selecting different soil types for experiments, and deepening the contribution of snow cover to the soil water are tasks that need further research in the future. At the same time, the sampling of deep soil can be increased further to study the contribution of snow melt water to deep soil water.

(3) There are also some conclusions about the dynamic characteristics of the stable isotope composition of hydrogen and oxygen in soil water. Ding et al. believed that the strong evaporation in arid regions led to the enrichment of heavy isotopes in soil water [65]. Jin et al. proposed to study the characteristics of soil water movement with the help of stable isotopes. The results showed that the influence of recharge water sources gradually weakened with the extension of time [1]. The results of this study show that with the increase of soil depth in spring, the average value of isotopes increases gradually, and the fluctuation of time change gradually decreases. The contribution rate and influence time of snow melt water to soil water have dynamic changes. Characteristically, the contribution of snowmelt water at the same depth decreased with the deepening of soil depth and the duration shortened. There are few studies on the contribution of snow melt water to soil water that are similar to this paper.

(4) The experimental design and sampling process in this study can be improved. The soil water of the soil in this study was probably affected by animal, plant, and microbial activities, which could not be separated and calculated temporarily, and this probably affected our results. The soil depth investigated in the experiments was not sufficient. By only obtaining soil samples from depths of 0–30 cm, the understanding of the specific penetration of the snowmelt water into the soil and its changes under different snow depths was not comprehensive. In addition, our findings were based on the type of soil in the experimental site, i.e., brown loam soil. Further studies should explore and demonstrate whether the contributions of the snowmelt water to other soil types and their dynamic changes are consistent. In addition, the melting time of the snow at different depths should be similar. When the 10 cm snow cover was fully melted, the contributions of the 30 cm and 50 cm snow covers to the soil water could not be evaluated because they were not completely melted. However, at this time, the contributions of the 30 cm and 50 cm snow covers to the soil water had already occurred. The contributions of the snow meltwater at different snow depths could only be compared after the 50 cm snow cover had completely melted, thus the contribution of the snowmelt water to the soil water could not be clarified. During the test, artificial snow accumulation was used for plots of different depths of snow to keep the snow density basically the same, but the uneven snow density during the artificial snow accumulation process would also affect the test results. In view of these limitations, the above problems and experimental results should be revised under more rigorous and controllable experimental conditions in the future.

(5) The stable isotopic composition of water is considered as the “fingerprint” of water, which records a large number of environmental information comprehensively reflecting the geochemical process of each system and connecting the characteristics of components in each link [66,67]. It plays an increasingly important role in the study of water cycle processes such as water source, migration and mixing. The most significant process of isotopic fractionation in nature mainly occurs in the evaporation condensation process of the transformation of liquid water and gaseous water. The isotopic fractionation effect is the internal cause of isotopic abundance distribution between gaseous water and liquid

water [68,69]. The experimental results of Ma Hongyun et al. showed that free air has a gradually increasing inhibitory effect on the enrichment process of evaporated water. In the process of evaporation, heavy water molecules such as HDO and H<sub>2</sub><sup>18</sup>O tend to enrich into liquid water; light water molecules such as H<sub>2</sub><sup>16</sup>O tend to enrich in gaseous water, which makes the abundance of heavy isotopes in evaporation residual water continue to increase [70]. Ma Hongyun et al. also proposed that air relative humidity is negatively correlated with the enrichment of hydrogen and oxygen stable isotopes in evaporated residual water. The greater the air humidity, the more unfavorable it is for the enrichment of body weight isotopes in residual water [71]. Therefore, we can also speculate that the factors unfavorable to evaporation will also lead to the enrichment of body weight isotopes of residual water. For example, the weaker the solar radiation and the stronger the pollution in the air, the weaker the evaporation of the water body will be. Therefore, the body weight isotope of residual water will be enriched, which will eventually affect the judgment of the water source and the contribution rate. At the same time, the black carbon pollution on the snow surface will reduce the albedo of the snow surface, increase the temperature of the snow surface, increase the evaporation of the snow surface, and reduce the isotopic enrichment of residual water. These are the next research issues.

## 5. Conclusions

(1) The oxygen isotope values in the snow at depths of 10 cm, 30 cm, and 50 cm have little difference. With the increase in soil depth, the hydrogen and oxygen isotope values show a gradual increase, and the isotopes in the soil water of the bare land are gradually enriched before the snow melts. The hydrogen and oxygen isotope values in snowfall and rainfall are quite different, and precipitation in different phases has a very significant impact on the isotope values.

(2) The different snow depths made different contributions to the soil moisture in the 0–30 cm soil layer. On average, the contributions of the 10 cm, 30 cm, and 50 cm snow depths to the soil moisture were 8.13%, 8.55%, and 11.24%, respectively. The contributions of the 10 cm, 30 cm, and 50 cm snow depths to the soil moisture at different soil depths were also different, i.e., the greater the snow depth, the greater the contribution. The retention time of the contribution to the 0–10 cm soil layer was the longest (average of 69 d), followed by that of the 20–30 cm soil layer (average of 59 d), while that of the 10–20 cm soil layer was the shortest (average of 54 d). The contributions of the different snow depths to the different soil layers decreased nearly linearly with time. The decay rates of the contributions to the 0–10 cm, 10–20 cm, and 20–30 cm soil layers were  $-0.33\%/d$ ,  $-0.37\%/d$ , and  $-0.26\%/d$ , respectively.

(3) The smaller the snow depth is, the more surface soil is mainly affected, while as the snow depth increases, it has a significant effect on the deep soil. Specifically, for 10 cm of snow water, it significantly affects the 0–10 cm soil layer; and when the snow cover is greater than 30 cm, it can affect the 20–30 cm soil layer.

(4) For every 1 mm increase in snow depth, the contribution rate of snowmelt water to soil water at different depths increases, while for every 1 mm increase in precipitation, the contribution rate to soil water at different depths decreases.

**Author Contributions:** Writing—original draft preparation, W.Z.; visualization, C.D.; writing—review and editing, L.Z.; resources, Y.T.; data curation, Y.H. and M.J. Besides, W.Z. and C.D. contributed equally to this work. All authors have read and agreed to the published version of the manuscript.

**Funding:** Natural Science Foundation of Heilongjiang Province of China (No. ZD2020D002). This research was funded by National Natural Science Foundation of China (Grant No. 41771067).

**Institutional Review Board Statement:** Not applicable.

**Informed Consent Statement:** Not applicable.

**Data Availability Statement:** The data is obtained and concluded by controlled outdoor experiments.

**Conflicts of Interest:** The authors declare that they have no conflict of interest.

## References

- Jin, Y.R.; Lu, K.X.; Li, P.; Wang, Q.; Zhang, T.G.; Liu, Y. Research on soil water movement based on stable isotopes. *Acta Pedol. Sin.* **2015**, *52*, 792–801.
- Chen, Y.N.; Li, Z.; Fan, Y.T.; Wang, H.J.; Fang, G.H. Research progress on the impact of climate change on water resources in the arid region of Northwest China. *Acta Geogr. Sin.* **2014**, *69*, 1295–1304.
- Ma, L.J.; Qing, D.H. Spatial-Temporal Characteristics of Observed Key Parameters for Snow Cover in China during 1957–2009. *J. Glaciol. Geocryol.* **2012**, *34*, 1–11.
- Jiang, L.; Zhu, F.S. China's Grain Production Status and Policy Suggestions in Major Grain Producing Areas. *Issues Agric. Econ.* **2015**, *36*, 17–24, 110. (In Chinese)
- Hu, C.L.; Li, J.; Jiao, M.; Wang, T.; Li, Y.H.; Lin, R.; Wang, Y. Change characteristics of shallow soil humidity and its impact climate factors in Liaoning spring sowing stage. *Agric. Res. Arid. Areas* **2018**, *36*, 277–283.
- Wang, Q.J.; Lv, J.J.; Li, X.F.; Wang, P.; Ma, G.Z. Distribution Characteristics of Heilongjiang Provincial Agricultural Meteorological Disasters and Effect on Agricultural Production. *Heilongjiang Hydraul. Sci. Technol.* **2016**, *44*, 57–61.
- Chen, H.; Zhang, L.J.; Li, W.L.; Zhang, J.F.; Gao, Y.H. Study on Risk Assessment and Zoning of Agricultural Arid Disaster in Heilongjiang Province. *Chin. Agric. Sci. Bull.* **2010**, *26*, 245–248.
- Liang, S. A study on Influence of Snow Cover on Soil Water and Heat in the Farmland in Northeast China. Master Thesis, Jilin University, Jilin, China, 2018.
- Sun, S.F. *Physics, Biochemistry and Parameterization of Land Surface Model*; China Meteorological Press: Beijing, China, 2005. (In Chinese)
- Li, Z.X.; Feng, Q.; Wang, Q.J.; Kong, Y.L.; Cheng, A.F.; Song, Y.; Li, Y.G.; Li, J.G.; Guo, X.Y. Contributions of local terrestrial evaporation and transpiration to precipitation using  $\delta^{18}\text{O}$  and D-excess as a proxy in Shiyang inland river basin in China. *Glob. Planet. Chang.* **2016**, *146*, 140–151.
- Penna, D.; Van Meerveld, H.J.; Zuecco, G.; Dalla Fontana, G.; Borga, M. Hydrological response of an alpine catchment to rainfall and snowmelt events. *J. Hydrol.* **2016**, *537*, 382–397. [[CrossRef](#)]
- Barbieri, M.; Nigro, A.; Petitta, M. Groundwater mixing in the discharge area of San Vittorino Plain (Central Italy): Geochemical characterization and implication for drinking uses. *Environ. Earth Sci.* **2017**, *76*, 393. [[CrossRef](#)]
- Xia, C.C.; Liu, G.D.; Meng, Y.C.; Wang, Z.Y.; Zhang, X.X. Impact of human activities on urban river system and its implication for water-environment risks: An isotope-based investigation in Chengdu, China. *Hum. Ecol. Risk Assess.* **2021**, *27*, 1416–1439. [[CrossRef](#)]
- El-Sayed, S.A.; Morsy, S.M.; Zakaria, K.M. Recharge sources and geochemical evolution of groundwater in the Quaternary aquifer at Atfih area, the northeastern Nile Valley, Egypt. *J. Afr. Earth Sci.* **2018**, *142*, 82–92. [[CrossRef](#)]
- Yang, N.; Wang, G.; Shi, Z.; Zhao, D.; Jiang, W.; Guo, L.; Liao, F.; Zhou, P.P. Application of multiple approaches to investigate the hydrochemistry evolution of groundwater in an arid region: Nomhon, Northwestern China. *Water* **2018**, *10*, 1667. [[CrossRef](#)]
- Zhou, P.P.; Li, M.; Lu, Y.D. Hydrochemistry and isotope hydrology for groundwater sustainability of the coastal multilayered aquifer system (Zhanjiang, China). *Geofluids* **2017**, *2017*, 7080346. [[CrossRef](#)]
- Kong, F.H.; Song, J.X.; Zhang, Y.; Fu, G.B.; Cheng, D.D.; Zhang, G.T.; Xue, Y. Surface Water-Groundwater Interaction in the Guanzhong Section of the Weihe River Basin, China. *Ground Water* **2019**, *57*, 647–660. [[CrossRef](#)]
- Wen, G.C.; Wang, W.K.; Duan, L.; Gu, X.F.; Li, Y.M.; Zhao, J.H. Quantitatively evaluating exchanging relationship between river water and groundwater in Bayin River Basin of northwest China using hydrochemistry and stable isotopes. *Arid. Land Geogr.* **2018**, *41*, 734–743.
- Yang, Y.G.; Xiao, H.L.; Wei, Y.P.; Zhao, L.J.; Zou, S.B.; Yin, Z.L.; Yang, Q. Hydrologic processes in the different landscape zones of Mafengou River basin in the alpine cold region during the melting period. *J. Hydrol.* **2011**, *409*, 149–156. [[CrossRef](#)]
- Li, Z.X.; Feng, Q.; Liu, W.; Wang, T.T.; Chen, A.F.; Gao, Y.; Guo, X.Y.; Pan, Y.H.; Li, J.G.; Guo, R.; et al. Study on the contribution of cryosphere to runoff in the cold alpine basin: A case study of Hulugou River Basin in the Qilian Mountains. *Glob. Planet. Chang.* **2014**, *122*, 345–361.
- Li, Z.X.; Feng, Q.; Liu, W.; Wang, T.T.; Gao, Y.; Wang, Y.M.; Cheng, A.F.; Li, J.G.; Liu, L. Spatial and temporal trend of potential evapotranspiration and related driving forces in Southwestern China, during 1961–2009. *Quat. Int.* **2014**, *336*, 127–144.
- Li, Z.X.; Feng, Q.; Wang, Q.J.; Song, Y.; Li, J.G.; Li, Y.G. The influence from the shrinking cryosphere and strengthening evapotranspiration on hydrologic process in a cold basin, Qilian Mountains. *Glob. Planet. Chang.* **2016**, *144*, 119–128.
- Penna, D.; Engel, M.; Mao, L.; Dell'Agnese, A.; Bertoldi, G.; Comiti, F. Tracer-based analysis of spatial and temporal variations of water sources in a glacierized catchment. *Hydrol. Earth Syst. Sci.* **2014**, *18*, 5271–5288. [[CrossRef](#)]
- Turner, K.W.; Wolfe, B.B.; Edwards, T.W. Characterizing the role of hydrological processes on lake water balances in the Old Crow Flats, Yukon Territory, Canada, using water isotope tracers. *J. Hydrol.* **2010**, *386*, 103–117. [[CrossRef](#)]
- Barbieri, M.; Ricolfi, L.; Battistel, M.; Nigro, A.; Garone, A.; Ferranti, F.; Sappa, G. Monitoring wetland deterioration in a coastal protected area in central Italy: Implications for management. *Euro-Mediterr. J. Environ. Integr.* **2019**, *4*, 1–10. [[CrossRef](#)]
- Krishan, G.; Vashisht, R.; Sudarsan, N.; Rao, M.S. Groundwater salinity and isotope characterization: A case study from South-West Punjab, India. *Environ. Earth Sci.* **2021**, *80*, 1–11. [[CrossRef](#)]

27. Krishan, G.; Prasad, G.; Anjali, K.C.P.; Patidar, N.; Yadav, B.K.; Kansal, M.L.; Singh, S.; Sharma, L.M.; Bradley, A.; Verma, S.K. Identifying the seasonal variability in source of groundwater salinization using deuterium excess—A case study from Mewat, Haryana, India. *J. Hydrol. Reg. Stud.* **2020**, *31*, 100724. [[CrossRef](#)]
28. Dincer, T.; Payne, B.R.; Florkowski, T.; Martinec, J.; Tongiorgi, E. Snowmelt runoff from measurements of tritium and oxygen-18. *Water Resour. Res.* **1970**, *6*, 110–124. [[CrossRef](#)]
29. Fritz, P.; Cherry, J.A.; Weyer, K.V.; Sklash, M.G. Storm runoff analyses using environmental isotope and major ions. In *Interpretation of Environmental Isotope and Hydrochemical Data in Groundwater Hydrology*; I.A.E.A.: Vienna, Austria, 1976; pp. 111–130.
30. Sklash, M.G. The Role of Groundwater in Storm and Snowmelt Runoff Generation. Ph.D. Thesis, University of Waterloo, Waterloo, ON, Canada, 1978.
31. Gui, J.; Li, Z.; Yuan, R.; Xue, J. Hydrograph Separation and the Influence from Climate Warming on Runoff in the North-Eastern Tibetan Plateau. *Quat. Int.* **2019**, *525*, 45–53. [[CrossRef](#)]
32. Li, Z.X.; Gui, J.; Wang, X.F.; Feng, Q.; Zhao, T.T.G.; Ouyang, C.J.; Guo, X.Y.; Zhang, B.J.; Shi, Y. Water resources in inland regions of central Asia: Evidence from stable isotope tracing. *J. Hydrol.* **2019**, *570*, 1–16. [[CrossRef](#)]
33. Sklash, M.G.; Farvolden, R.N. The role of groundwater in storm runoff. *Dev. Water Sci.* **1979**, *12*, 45–65.
34. Hooper, R.P.; Christophersen, N.; Peters, N.E. Modelling streamwater chemistry as a mixture of soilwater end-members—An application to the Panola Mountain catchment, Georgia, USA. *J. Hydrol.* **1990**, *116*, 321–343. [[CrossRef](#)]
35. Hooper, R.P. Diagnostic tools for mixing models of stream water chemistry. *Water Resour. Res.* **2003**, *39*, 1055. [[CrossRef](#)]
36. Yao, T.D.; Valerie, M.V.; Gao, J.; Yu, W.S.; Yang, X.X.; Risi, C. A review of climatic controls on  $\delta^{18}\text{O}$  in precipitation over the Tibetan Plateau: Observations and simulations. *Rev. Geophys.* **2013**, *51*, 525–548. [[CrossRef](#)]
37. Yu, W.S.; Yao, T.D.; Lewis, S.; Tian, L.; Ma, Y.M.; Xu, B.Q.; Qu, D.M. Stable oxygen isotope differences between the areas to the north and south of Qinling Mountains in China reveal different moisture sources. *Int. J. Climatol.* **2014**, *34*, 1760–1772. [[CrossRef](#)]
38. Jouzel, J.; Souchez, R.A. Melting–refreezing at the glacier sole and the isotopic composition of the ice. *J. Glaciol.* **1982**, *28*, 35–42. [[CrossRef](#)]
39. Hren, M.T.; Bookhagen, B.; Blisniuk, P.; Booth, A.L.; Chamberlain, C.P.  $\delta^{18}\text{O}$  and  $\delta\text{D}$  of streamwaters across the Himalaya and Tibetan Plateau: Implications for moisture sources and paleoelevation reconstructions. *Earth Planet. Sci. Lett.* **2009**, *288*, 20–32. [[CrossRef](#)]
40. Zhang, S.; Yu, W.X.; Zhang, Q.L. The distribution of deuterium and heavy oxygen in snow and ice, in the Jolmo Lungma regions of the southern Tibet. *Sci. China B* **1973**, *4*, 430–433.
41. Pang, H.X.; He, Y.Q.; Theakstone, W.H. Soluble ionic and oxygen isotopic composition of a shallow firn profile, Baishui Glacier No.1, southeastern Tibetan Plateau. *Ann. Glaciol.* **2007**, *46*, 325–330. [[CrossRef](#)]
42. Karim, A.; Veizer, J. Water balance of the Indus River Basin and moisture source in the Karakoram and western Himalayas: Implications from hydrogen and oxygen isotopes in river water. *J. Geophys. Res. Atmos.* **2002**, *107*, 1–9. [[CrossRef](#)]
43. Quade, J.; Garzzone, C.; Eiler, J. Paleoelevation reconstruction using pedogenic carbonates. *Rev. Mineral. Geochem.* **2007**, *6*, 53–87. [[CrossRef](#)]
44. Chen, K.; Meng, Y.; Liu, G.; Xia, C. Analysis for effects of monsoon activities on oxygen and hydrogen isotopes variation based on Hong Kong GNIP long-term data. *J. Radioanal. Nucl. Chem.* **2021**, *328*, 1055–1068. [[CrossRef](#)]
45. Li, P.; Wu, J.; Qian, H. Preliminary assessment of hydraulic connectivity between river water and shallow groundwater and estimation of their transfer rate during dry season in the Shidi River, China. *Environ. Earth Sci.* **2016**, *75*, 1–16. [[CrossRef](#)]
46. Song, X.F.; Wang, S.Q.; Xiao, G.Q.; Wang, Z.M.; Liu, X. Time Series Analysis of Soil Water Dynamics in the Shallow Groundwater Areas of North China Plain. *J. Nat. Resour.* **2011**, *26*, 145–155.
47. Xu, Y.D.; Wang, J.K.; Gao, X.D.; Zhang, Y.L. Application of Hydrogen and Oxygen Stable Isotope Techniques on Soil Water Research: A Review. *J. Soil Water Conserv.* **2018**, *32*, 1–9, 15.
48. Xiao, D.A.; Wang, S.J. Comments on the progress and direction in soil water research. *Ecol. Environ. Sci.* **2009**, *18*, 1182–1188.
49. Zhang, X.J.; Song, W.F.; Wu, J.K.; Wang, Z.J. Characteristics of Hydrogen and Oxygen Isotopes of Soil Water in the Water Source Area of Yuanyang Terrace. *Environ. Sci.* **2015**, *36*, 2102–2108.
50. Wu, Y.J.; Du, T.S. Stable Hydrogen and Oxygen Isotopic Distributions and Water Movement in the Soil Under Plastic Film-mulching Furrow Irrigation. *China Rural. Water Hydropower* **2016**, *9*, 73–76.
51. Wu, W.; Jiang, Y.J.; Jia, Y.N.; Peng, X.Y.; Duan, S.H.; Liu, J.C.; Wang, Z.X. Temporal and Spatial Distribution of the Soil Water  $\delta\text{D}$  and  $\delta^{18}\text{O}$  in a Typical Karst Valley: A Case Study of the Zhongliang Mountain, Chongqing City. *Environ. Sci.* **2018**, *39*, 5418–5427.
52. Robertson, J.A.; Gazis, C.A. An oxygen isotope study of seasonal trends in soil water fluxes at two sites along a climate gradient in Washington state (USA). *J. Hydrol.* **2006**, *328*, 375–387. [[CrossRef](#)]
53. Fu, Q.; Hou, R.J.; Wang, Z.L.; Li, T.X. Soil moisture thermal interaction effects under snow cover during freezing and thawing period. *Trans. Chin. Soc. Agric. Eng.* **2015**, *31*, 101–107, (In Chinese with English abstract).
54. Fu, Q.; Hou, R.J.; Liu, D.; Li, T.X.; Wang, Z.L. Spatial distribution of soil moisture content under condition of snowcover. *Trans. Chin. Soc. Agric. Eng.* **2016**, *32*, 120–126, (In Chinese with English abstract).
55. Lu, L.; Liu, J.H.; Ye, R.; Li, W.; Qin, D.Y. Preliminary Study on Relationship between Snow Covers and Soil Moisture in North China. *Water Sav. Irrig.* **2011**, *1*, 10–13, 17, (In Chinese with English abstract).
56. Liang, S.; Li, X.; Zheng, X.; Jiang, T.; Qiao, D. Effects of winter snow cover on spring soil moisture based on remote sensing data product over farmland in northeast China. *Remote Sens.* **2020**, *12*, 2716. [[CrossRef](#)]

57. Možný, M.; Hájková, L.; Tolasz, R. Influence of Snow Cover on Soil Moisture and Frost Dynamics in Winter of 2016–2017 in Czech Republic. In Proceedings of the ‘Snow an ecological phenomenon’, Smolenice, Slovakia, 19–21 September 2017.
58. Sun, N.X. Study on Field Water Transformation Using Isotopes: A Case of Daxing District, Beijing. Master Thesis, China University of Geosciences, Beijing, China, 2015.
59. Dansgaard, W. The abundance of  $^{18}\text{O}$  in atmospheric water and water vapor. *Tellus* **1953**, *5*, 461–469. [[CrossRef](#)]
60. Vodila, G.; Palcsu, L.; Futó, I.; Szántó, Z. A 9-year record of stable isotope ratios of precipitation in Eastern Hungary: Implications on isotope hydrology and regional palaeoclimatology. *J. Hydrol.* **2011**, *400*, 144–153. [[CrossRef](#)]
61. Negrel, P.; Petelet-Giraud, E.; Millot, R. Tracing water cycle in regulated basin using stable  $\delta^{18}\text{O}$ – $\delta^2\text{H}$  isotopes: The Ebro river basin (Spain). *Chem. Geol.* **2016**, *422*, 71–81. [[CrossRef](#)]
62. Ma, J.; Song, W.F.; Wu, J.K.; Wang, Z.J.; Zhang, X.J.; Liu, Z.B. Characteristics of Hydrogen and Oxygen Isotopes of Precipitation and Soil Water in Woodland in Water Source Area of Yuanyang Terrace. *J. Soil Water Conserv.* **2016**, *30*, 243–248, 254.
63. Gazis, C.; Feng, X. A stable isotope study of soil water: Evidence for mixing and preferential flow paths. *Geoderma* **2004**, *119*, 97–111. [[CrossRef](#)]
64. Zhang, L.J.; Wang, C.Z.; Li, Y.S.; Huang, Y.T.; Zhang, F.; Pan, T. High-latitude snowfall as a sensitive indicator of climate warming: A case study of Heilongjiang Province, China. *Ecol. Indic.* **2021**, *122*, 107249. [[CrossRef](#)]
65. Ding, J.; Liu, Y.F.; Wang, J.J. Dynamic Variation characteristics of Hydrogen and Oxygen Stable Isotope Composition in Soil Water after Salt Water Irrigation in Arid Area. *Saf. Environ. Eng.* **2020**, *27*, 32–39.
66. Panichi, C.; Gonfiantini, R. Environmental isotopes in geothermal studies. *Geothermics* **1977**, *6*, 143–161. [[CrossRef](#)]
67. Vimeux, F.; Masson, V.; Jouzel, J.; Petit, J.R.; Steig, E.J.; Stievenard, M.; Vaikmae, R.; White, J.W.C. Holocene hydrological cycle changes in the Southern Hemisphere documented in East Antarctic deuterium excess records. *Clim. Dyn.* **2001**, *17*, 503–513. [[CrossRef](#)]
68. Craig, H.; Gordon, L.I.; Horibe, Y. Isotopic exchange effects in the evaporation of water: 1. Low-temperature experimental results. *J. Geophys. Res.* **1963**, *68*, 5079–5087. [[CrossRef](#)]
69. Gat, J.R. Isotope composition of air moisture over the Mediterranean Sea: An index of the air-sea interaction pattern. *Tellus Ser. B-Chem. Phys. Meteorol.* **2003**, *55*, 953–965. [[CrossRef](#)]
70. Ma, H.Y.; Wang, X.Y.; Zhang, J.; Huang, J.T.; Yin, L.H.; Dong, J.Q. An Experimental Study of The Isotopic Enrichment of Evaporating Water. *Water Sav. Irrig.* **2014**, 36–39, (In Chinese with English abstract).
71. Ma, H.Y.; Yin, L.H.; Zhang, J.; Huang, J.T.; Wang, X.Y.; Dong, J.Q. The impact of free air humidity on the fractionation in the process of evaporation. *Geol. Bull. China* **2015**, *34*, 2087–2091, (In Chinese with English abstract).